Submitted to *Int. Conf. on Brain Processes, Theories and Models. W.S. McCulloch: 25 Years in Memoriam*, Nov. 1995

Hysteresis and Asymmetric Sensitivity to Change in Pacemaker Responses to Inhibitory Input Transients

Michael Stiber* *and* Ricci Ieong*

Technical Report HKUST-CS95-29
June 1995

* Department of Computer Science
The Hong Kong University of Science & Technology
Clear Water Bay, Kowloon, Hong Kong
stiber@cs.ust.hk
ricci@cs.ust.hk

Abstract

The coding of presynaptic spike trains to postsynaptic ones is the unit of computation in nervous systems. While such coding has been examined in detail under stationary input conditions, the effects of changing inputs have until recently been understood only superficially. When a neuron receives transient inputs with monotonically changing instantaneous rate, its response along time depends not only on the rate at that time, but also on the sign and magnitude of its rate of change. This has been shown previously for the living embodiment of a prototypical inhibitory synapse. We present simulations of a physiological model of this living preparation which reproduce its behaviors. Based on these results, we propose a simple model for the neuron's response involving a constant delay between its input and internal state. This is then generalized to a nonlinear dynamical model of any similar system with an internal state which lags its input.

The Hong Kong University of Science & Technology
Technical Report Series
Department of Computer Science

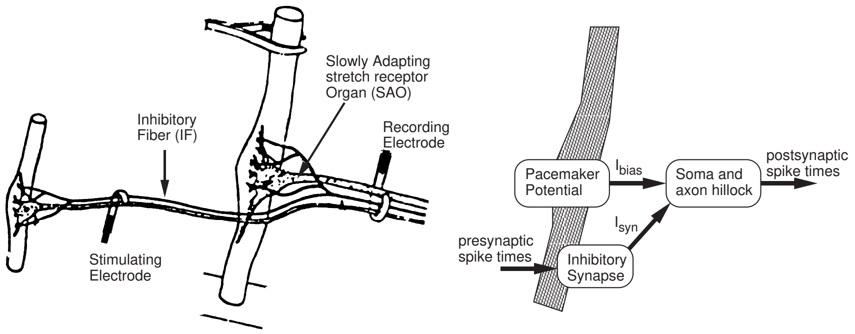

Figure 1: The crayfish stretch receptor experimental setup (left) and the modified permeability model (right).

1 Introduction

One of the most important functions of any animal's nervous system must be modifying its actions based on changing conditions in its surrounding environment. For such modification to take place, environmental changes must be encoded as changes in the spike trains produced by some neurons in the appropriate sensorimotor systems. Motor activity must also be encoded as changes in neural discharges. Considering the prevalence of such changes, one can only conclude that neurons' encoding of changing inputs to their outputs is the norm rather than the exception.

From the point of view of understanding the encoding process, however, it is far easier to analyze neurons' responses to stationary inputs than nonstationary ones. This difficulty is reflected in the superficiality of understanding the effects of input transients on neuron behavior [4]. Our present purpose is to extend previous work on synaptic coding of stationary, pacemaker spike trains [7, 5, 6, 10] to transient spike trains in which presynaptic rate changes monotonically [8]. Previous experiments on a living preparation indicate that not only is instantaneous presynaptic rate reflected in its responses, but also the sign and magnitude of the rate of change of presynaptic rate [8]. To our knowledge, the only other work on coding of presynaptic transients has involved the aftereffects of step-like changes in presynaptic rate.

In this communication, we briefly summarize previous findings from a living preparation (the crayfish slowly adapting stretch receptor organ, or SAO, shown in Fig. 1(left)) [8] and show similar results obtained from a model of that preparation (right) [3, 9]. In both cases, we are dealing with the embodiment of a prototypical inhibitory synapse, and conclusions derived from them should be acceptable, as a working hypothesis at least, for other preparations. We then treat in some detail the questions of how a neuron's responses change as input changes become more and more abrupt, and how its responses also reflect accelerating versus decelerating presynaptic discharges.

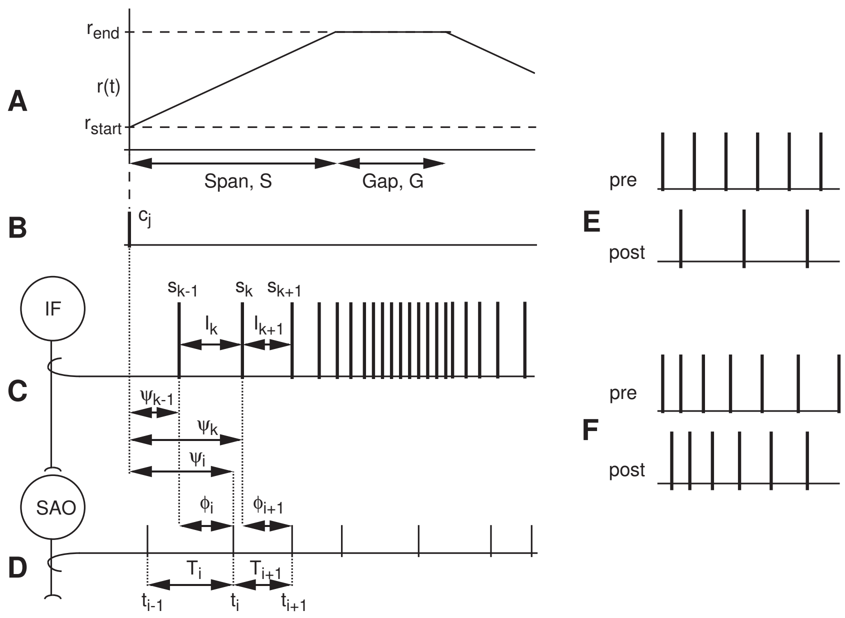

Figure 2: Transient generation and definition of terms.

2 Methods

As shown in Fig. 1, the experimental preparations involved a postsynaptic neuron and an experimenter-controlled presynaptic discharge applied through an inhibitory synapse. When no inputs are applied, the postsynaptic neuron produces spikes as a *pacemaker*, with all interspike intervals nearly equal to N, its *natural* interval. The presynaptic discharges were controlled as described in section 2.1, and times of occurrence of presynaptic and postsynaptic events were recorded for analysis (section 2.2) using tools and concepts from the field of Nonlinear Dynamics.

2.1 Transient Generation

Fig. 2(A–D) illustrates how transients were generated and data collected. In (A), an instantaneous *rate control waveform*, $r(t)$, was selected to produce mirror-image transients which accelerated monotonically from an initial rate, r_{start}, to a final rate, r_{end}, over a length of time termed the transient's *span*, S. After a *gap*, G, long enough to separate the aftereffects of one transient to another, the instantaneous rate decelerated from r_{end} back to r_{start}. This sequence repeat after another gap for the duration of a trial. Presynaptic intervals were computed in the simulations as $s_k = s_{k-1} + 1/r(s_{k-1})$, where k is a counter of presynaptic spikes ($k = 1, 2, \ldots$) and s_k is the time of the k^{th} presynaptic spike (as shown in Fig. 2(C)).

Besides the presynaptic spikes at times s_k, the two other events of note here are the postsynaptic spikes (D), occurring at times t_i ($i = 1, 2, \ldots$), and the *cycle markers* (B) at times c_j ($j = 1, 2, \ldots$) — the latter being "artificially" introduced events marking the start of each pair of transients.

2.2 Analysis

Analysis was based on certain interspike intervals and cross-intervals between spike trains. These were computed from a *reference event* back to some other event, and therefore we use as a subscript for an interval the subscript of its reference event, and include:

- presynaptic intervals $I_k = s_k - s_{k-1}$ are shown in (C); they are the reciprocals of $r(s_{k-1})$,
- postsynaptic intervals, $T_i = t_i - t_{i-1}$ (D),
- cross intervals or *phases*, $\phi_i = t_i - s_*$ (D), the interval from a postsynaptic spike back to the most recent preceding presynaptic one, s_*,
- cross intervals $\psi_i = t_i - c_*$ and $\psi_k = s_k - c_*$ (C), from a post- or presynaptic spike, respectively, back to the most recent preceding cycle marker, c_*.

2.2.1 Basic and Pooled Graphs

Using these intervals, phases, and cross intervals, graphs can be constructed to clearly identify neuronal responses. Fig. 3 shows the two graphs that we will be concerned with here. On top is the *basic graph*, which is merely a plot of interval or phase versus time. Points in an interval plot are (t_i, T_i); those in a phase plot are (t_i, ϕ_i).

Also shown in the figure are those segments of ongoing time which correspond to the spans of transients; points which occur in each of the two transients are either filled completely or half-way, while points outside the spans of transients are unfilled. This makes the construction of the *pooled graph*, shown in the bottom of the figure, apparent. A pooled graph is a plot of interval or phase versus cross interval to the most recent cycle marker. It is as though the basic plot were cut into segments that correspond to transients and then those segments were stacked on top of each other. Points in a pooled graph are (ψ_i, T_i) or (ψ_i, ϕ_i), for $0 \leq \psi_i \leq S$ (accelerating transients) or $S + G \leq \psi_i \leq 2S + G$ (decelerating ones).

2.2.2 Categorization of Dynamical Behavior

A neuron's output, like that of other nonlinear dynamical systems, is a function not only of its input but also of its internal state. Moreover, its response to linear combinations

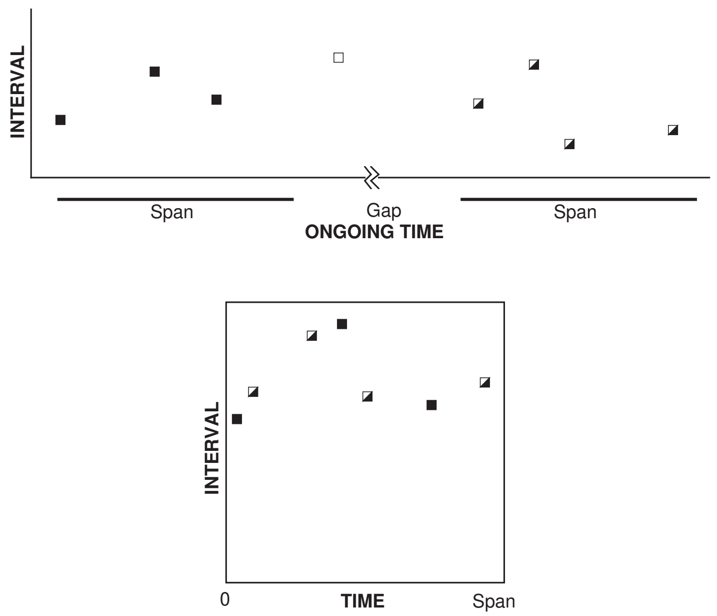

Figure 3: Basic and pooled graphs.

of different inputs is typically not a linear combination of its responses to each taken separately. This is true for even slight changes of input: for instance, its response to pacemaker inputs with $I_k = I = 100$ms might be drastically different from that with pacemaker input at $I = 101$ms. Because of the complex input/output relationship, we must define a neuron's input/output behavior in terms of *attractors* and *bifurcations*.

The concept of an attractor deals with the issue of the system's internal state. We can view the internal state at any time as a point in a *state space*, the axes of which are the state variables of the system. In the state space, the system's state point traces out some *trajectory* as time progresses. For stationary behaviors, this trajectory describes some topological entity: the attractor.

Different stationary behaviors correspond to different kinds of attractors. A pacemaker's state follows a closed loop in its state space: a limit cycle. Other *periodic* or repeating behaviors may involve more than one interval, and correspond to trajectories that loop around more than once before closing back on themselves. In the current setup, we define a general stationary periodic behavior as *p:q locking*, where p presynaptic spikes occur in the same time frame as q postsynaptic spikes (p, q integers). Being periodic, the sequences of intervals $\langle T_i, T_{i+1}, \ldots, T_{i+q-1}\rangle$ and phases $\langle \phi_i, \phi_{i+1}, \ldots, \phi_{i+q-1}\rangle$ repeat: $T_i = T_{i+q}$ and $\phi_i = \phi_{i+q}$. Fig. 2(E) illustrates 2:1 locking.

There are also aperiodic behaviors: for our purposes here, it suffices to say that the trajectories traced out by the state over time do not connect back on themselves and thus their sequences of intervals and phases do not repeat. There are also counterparts of these stationary behaviors for the nonstationary inputs used here: *alternation* is the class of behaviors which includes both stationary and nonstationary "lockings". Fig. 2(F) shows an example of 1:1 alternation with a decelerating presynaptic discharge.

For any input interval I_k there is an associated behavior, be it periodic or aperiodic. As I_k changes, the neuron's behavior may change in on of two ways: *quantitatively* or *qualitatively*. An example of a quantitative change would be a change from 1:1 locking with $T_i = 100$ms to 1:1 locking with $T_i = 110$ms. A qualitative change is a change from one type of behavior to another, such as from 1:1 locking to an aperiodic behavior. This latter change is only possible in nonlinear systems, and a description of the dependence of behavior type on some control parameter is termed the system's *bifurcation behavior*. Any value of the control parameter at which two different behaviors come together (where a qualitative change occurs) is a *bifurcation point*.

In our pooled graphs, we are plotting a measure of the neuron's response, T_i or ϕ_i, versus time since the beginning of any transient, ψ_i. Since $r(\psi_i)$ uniquely determines the instantaneous input rate at that time, a pooled graph is a plot of system behavior versus input rate, where input rate is the control parameter. Thus, a pooled graph can be treated as a *bifurcation diagram*: a plot of the bifurcation behavior of a system.

2.2.3 Bifurcation Point Determination

Pooled graphs were generated for accelerating and decelerating ramp transients with slopes $m = (r_{\text{end}} - r_{\text{start}})/S$ varying from slow (0.5 Hz/s) to fast (near 20 Hz/s). For each pooled graph, we located the instantaneous rates at which certain key bifurcations occurred. For the purposes of gathering the preliminary data reported here, the bifurcation points at either end of $1:1$ alternation were determined by hand measurement from the pooled graphs, and converted to instantaneous input rates. Work is currently underway to locate more bifurcation points with greater accuracy.

3 Results

Fig. 4 presents phase pooled graphs which show typical responses of the model (left) and SAO (right) to a slowly accelerating ramp ($m = 0.8$Hz/s). Most apparent are the distinct signatures of alternating and non-alternating behaviors and the bifurcations between behaviors. In a $p{:}q$ alternating behavior, there are precisely q categories of ϕ, and this produces in the pooled graph q narrow horizontal bands at their values (which change smoothly as the inputs accelerate). On the other hand, non-alternating behaviors (with some exceptions which we shall ignore here) do not have discrete phase values and therefore do not produce narrow horizontal bands in the pooled graph.

Bifurcation points are values of ψ_i at which two different behaviors come together. This

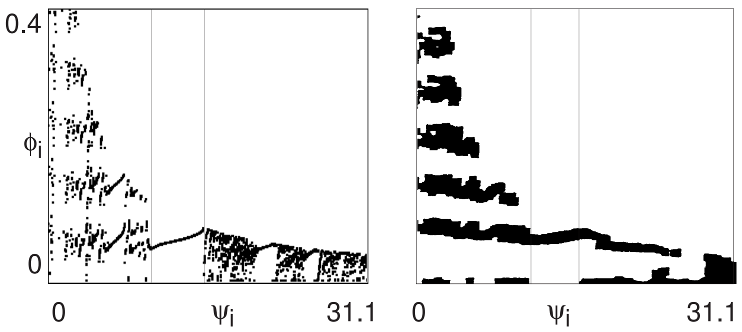

Figure 4: Phase pooled graphs showing transient responses of SAO (right) and simulation (left). Transient was accelerating ramp, 39ms $\leq I_k \leq$ 1.667s, S = 31.1s. Natural firing interval N = 84ms.

can be seen in the graphs as values where one of the phase categories of an alternation disappears (along increasing ψ_i), or where the compact phase categories of alternation are replaced by the vertically dispersed points of a non-alternating behavior (or vice versa). Two bifurcation points in particular are indicated in the graphs by thin vertical lines, corresponding to the minimum and maximum values of ψ_i which bound 1:1 alternation.

Several simulations were conducted with m covering a range of values from slow ones like that shown in Fig. 4 to fast ones near 20Hz/s. Fig. 5 plots the bifurcation points bounding 1:1 alternation (as instantaneous input rate) versus $|m|$ for both accelerating and decelerating ramp transients. Bifurcation points for pacemaker driving are also plotted. There is a clear dependence of bifurcation point location on the magnitude and sign of m, with more steeply accelerating transients producing bifurcations at higher rates; decelerating ones at lower rates. As $|m| \rightarrow 0$, the transient bifurcation points converge to the stationary ones. This is the asymmetric sensitivity to change which has been seen in the living preparation. The fact that the same bifurcation occurs at different instantaneous rates if the transient is accelerating versus decelerating produces hysteresis (indicated for one value of m by H in the figure).

Fig. 5 also includes lines of best fit for each set of bifurcation points; Table 1 lists their correlation coefficients as well as other information which is discussed in the next section.

4 Discussion

It is important to reiterate that both the living preparation and the model are prototypes of synaptic coding across inhibitory synapses, and therefore our results here should be assumed widely applicable in the absence of evidence to the contrary. However, an even more general model of transient coding can be formulated to explain the results in the previous section.

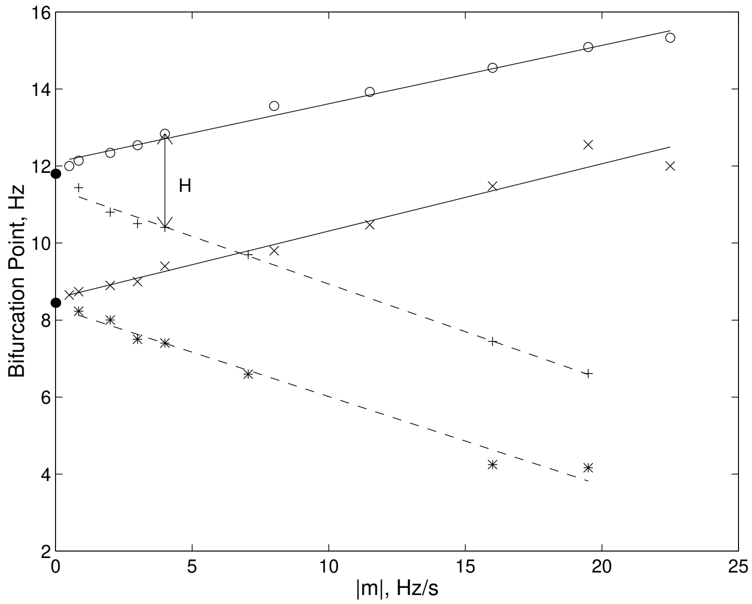

Figure 5: Bifurcation points bounding 1:1 alternation for accelerating ($\circ$, $\times$) and decelerating ($+$, $*$) transients. Lines of best fit shown as solid and dashed, respectively. Hysteresis (H) caused by non-coincident bifurcations. Actual bifurcation points under pacemaker driving indicated at $|m| = 0$ ($\bullet$).

One simple way to model the neuron's transient response is illustrated in Fig. 6. In this model, we assume that the neuron is composed of a pure linear system that introduces a delay δ, coupled to a nonlinear system which, based on the delayed input, selects an attractor from the neuron's repertoire. This is essentially what has been proposed previously (as a "first order lead-lag" behavior) to explain the observed hysteresis in the SAO [8]. If the input is the instantaneous presynaptic inhibitory rate, $r(t)$, the delayed version is an

Table 1: Delays computed from the slopes of the lines in Fig. 5. Also y-intercepts of lines, actual bifurcation points for stationary (pacemaker, $|m| = 0$) driving, and correlation coefficients.

Curve	$\delta(ms)$	y-int (Hz)	Bif. pt. (Hz)	r
$\circ$	152	12.1	11.8	0.9941
$+$	247	11.4		0.9975
$\times$	175	8.57	8.45	0.9823
$*$	231	8.32		0.9908

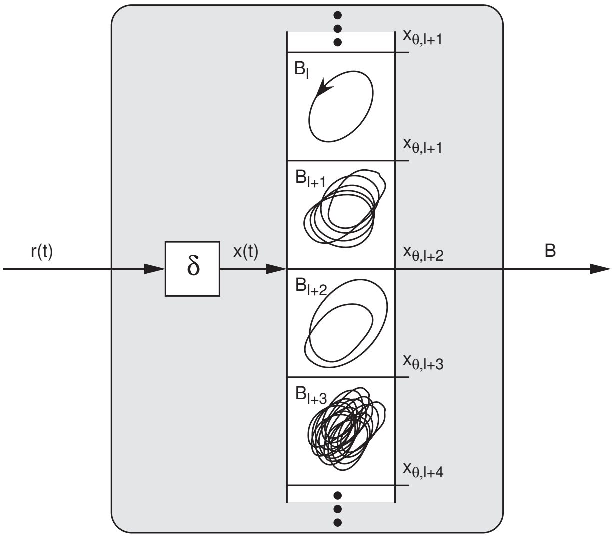

Figure 6: Pure delay model of neural responses.

internal state of the system, $x(t) = r(t-\delta)$, and attractor selection takes place by comparing $x(t)$ to an ordered set of boundary values (bifurcation points) $\{x_{\theta_\ell}\}$ ($\ell = 1, 2, \ldots$). The output behavior B corresponds to the attractor between bifurcations $\ell + m$ and $\ell + m + 1$ when $x_{\theta_{\ell+m}} \leq x(t) \leq x_{\theta_{\ell+m+1}}$ (for some integer m).

The mechanism by which this pure delay could cause hysteresis is presented in Fig. 7. In (A), $r(t)$ and $x(t)$ are plotted on the same axes, the former as a thin solid line and the latter as a dashed line. Let's say that the neuron will switch from one behavior to another when $x(t)$ passes through x_θ in either direction. However, we can't record $x(t)$; we can only record $r(t)$. Therefore, just as we have done here using the pooled graphs, we can determine $r_{\theta+}$ and $r_{\theta-}$, the instantaneous presynaptic rates which correspond to the same bifurcation point, with the former during acceleration and the latter during deceleration. The bifurcation value for stationary pacemaker driving can be termed r_θ or x_θ.

This behavior is replotted in a more familiar form in Fig. 7(B). The neuron is viewed as a bistable system, existing in one of two states (corresponding to the two behaviors B_1 and B_2) which come together at the bifurcation point. Since $r_{\theta+} > r_{\theta-}$, the neuron displays hysteresis, switching from B_1 to B_2 at $r_{\theta+}$ when accelerating (moving to the right), and from B_2 to B_1 at $r_{\theta-}$ (moving to the left). The amount of hysteresis, or displacement of $r_{\theta+}$ and $r_{\theta-}$ from r_θ, is trivially computed from (A) by noticing that the slope of $r(t)$ is $m_+ = (r_{\theta+} - r_\theta)/\delta$ and $m_- = (r_{\theta-} - r_\theta)/\delta$. Since m is a control parameter, and $r_{\theta+}$ and $r_{\theta-}$ are measurable quantities, we can determine δ from Fig. 5 using the method shown in Fig. 7(C): find the best-fitting line to the plot of r_θ versus $|m|$, and then δ is the absolute value of the slope of that line (e.g., $\mathrm{d}r_\theta/\mathrm{d}|m|$). Values of δ obtained from Fig. 5 are listed in table 1.

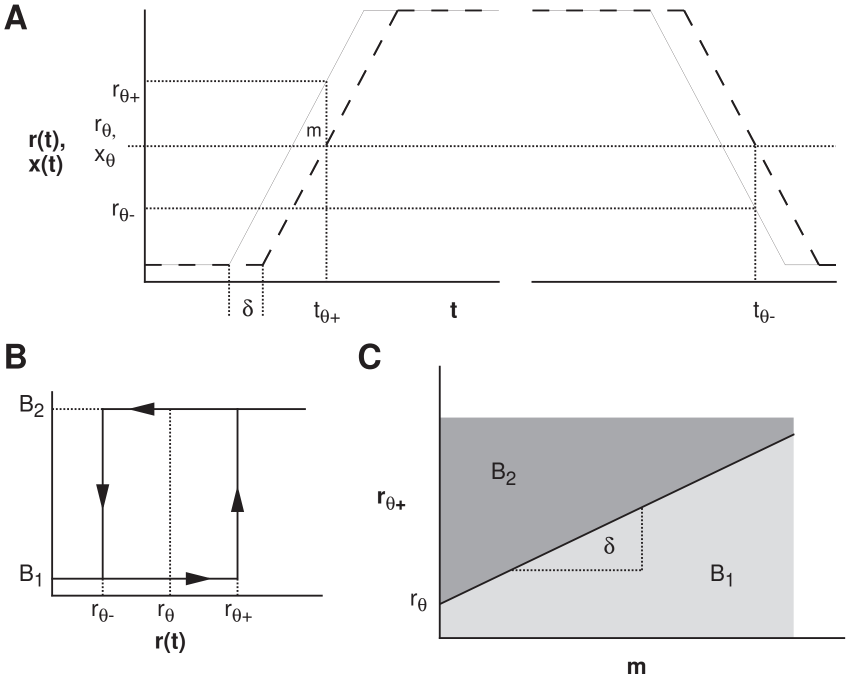

Figure 7: Realization of hysteresis caused by delay and computation of δ.

From the correlation coefficients in the table, we conclude that a constant delay is consistent with the data over most of the range of m explored. There are a couple important exceptions, however. First of all, the y-intercepts of the lines of best fit for accelerating and decelerating bifurcations bracket the stationary bifurcations. From this and visual inspection of Fig. 5, we suggest that the delay is not constant for small m, and is in fact larger for values below 1Hz/s. Second, while the slopes of the two accelerating lines are roughly equal (and also the two decelerating lines), they are not the same for acceleration and deceleration. Therefore, we conclude that asymmetric sensitivity to change cannot be explained solely in terms of a constant delay in the response of the neuron to changing input: in fact, the neuron model seems to respond more rapidly to accelerating than to decelerating instantaneous rates.

Based on a method for constructing complex attractors from simpler components proposed by Deng [2], Fig. 8 shows one way to visualize the hysteresis and sensitivity to rate of change displayed by the neuron. The figure shows a "twisted staircase" in 3 dimensions, with the $r(t)$ axis left/right, $|m|$ into and out of the page, and the z axis not meant to correspond to any physical parameter. Each "step" of the staircase corresponds to the range of parameters in which a particular set of qualitatively similar behaviors (such as 1:1 alternation) exists; "risers" connect steps at bifurcation points. Thus, every point on every step corresponds to a particular behavior, with the attractor "icons" drawn there merely

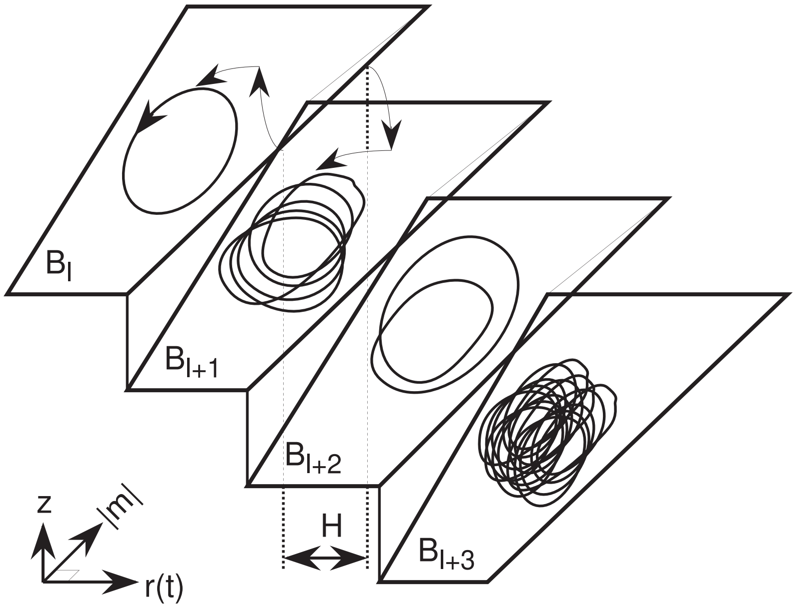

Figure 8: A "twisted staircase" model of asymmetric sensitivity to rate of change.

indicating the qualitative change between steps.

For $|m| = 0$, the risers form right angles to the steps, and the bifurcation points are unique. As $|m|$ increases, bifurcation points for $m > 0$ and $m < 0$ diverge, the risers no longer form right angles to the steps, and the bifurcation points for accelerating inputs (walking "down" the stairs) no longer correspond to those for decelerating ones (walking "up" the stairs). Viewed from above, the pairs of bifurcations bounding any behavior would correspond to the graph in Fig. 5.

One example is shown in the figure by the curves and arrows. As $r(t)$ increases, the neuron shifts from behavior B_ℓ to $B_{\ell+1}$, and then over some period of time its trajectory converges towards the type of attractor that corresponds to $B_{\ell+1}$. Moving the other way, as $r(t)$ decreases the system shifts from $B_{\ell+1}$ to B_ℓ at a lower value of $r(t)$. Hence, the hysteresis indicated by H.

Beyond its visual appeal, this formulation can also explain why some behaviors disappear as $|m|$ increases. There are two possibilities. If the slopes of the bifurcation lines for different bifurcations are not equal, then it is possible that, for large $|m|$, one step will completely overlap another, so that a point moving off the edge of one will skip the next step entirely. This would result in the system moving from, for example, B_ℓ directly to $B_{\ell+2}$ without passing through $B_{\ell+1}$.

Even if delays are constant for all bifurcations, there is still the effect of *residence time* on each step to consider. As $|m|$ increases, $r(t)$ changes more rapidly: we no longer "walk" up and down the stairs; we "run". Constant delay would mean that all accelerating bifurcations form parallel lines along the $|m|$ axis: the width of a step between bifurcations in terms of range of $r(t)$ would be constant, but *decreasing* in terms of range of t. The neuron would spend less time on each step (since different steps are different widths, the exact amount of time would depend on the particular step). Since it takes a finite amount of time for the state trajectory to converge close enough to an attractor for a behavior to be recognizable, for some behaviors there may not be enough time for this to happen. These behaviors would be abolished, replaced by short, trendy discharges between other, still-recognizable behaviors.

5 Conclusions

We started this paper off by asking questions of why a neuron shows hysteresis and asymmetric sensitivity to monotonic changes in presynaptic rate. To investigate this is more detail than practical with the living preparation, a physiological model was introduced which reproduces its behaviors well. The responses of this model to changing rate of change of instantaneous input rate are explained, with some reservations, by a model in which the neuron's internal state lags behind its input by some constant delay. This in turn suggested a dynamical model of how bifurcation points vary with increasing input transient slope. Based on this model, we can predict mechanisms for the abolition of certain behaviors, which can occur even if the neuron's internal state's lag is not strictly a constant — it merely needs to be non-decreasing.

The behaviors and characteristics of nonlinear dynamical systems are *universal*, in that lessons learned from systems as diverse as chemical reactions, fluid flow, lasers, neurons, etc. [1] can be applied almost directly to each other. This ability to go from specific example to general principle suggests that the results presented here have applicability beyond this living preparation, regardless of its prototypical nature.

Acknowledgements

The authors would like to thank José P. Segundo for furnishing data for use in this project, and Dominic Lai and Ng Ka Ho for their programming help. Support for this work was provided by the Hong Kong Research Grants Council (CERG HKUST187/93E).

References

[1] P. Bergé, Y. Pomeau, and C. Vidal, *Order Within Chaos: A Deterministic Approach to Turbulence.* New York: Wiley, 1986.

[2] B. Deng, "Constructing homoclinic orbits and chaotic attractors," *Int. J. Bifurcation and Chaos*, vol. 4, no. 4, pp. 823–41, 1994.

[3] A. Edman, S. Gestrelius, and W. Grampp, "Analysis of gated membrane currents and mechanisms of firing control in the rapidly adapting lobster stretch receptor neurone," *J. Physiol.*, vol. 384, pp. 649–69, 1987.

[4] B. Huberman and W. Wolff, "Finite precision and transient behavior," *Phys. Rev. A*, vol. 32, pp. 3768–70, 1985.

[5] J. P. Segundo, E. Altshuler, M. Stiber, and A. Garfinkel, "Periodic inhibition of living pacemaker neurons: I. Locked, intermittent, messy, and hopping behaviors," *Int. J. Bifurcation and Chaos*, vol. 1, pp. 549–81, September 1991.

[6] J. P. Segundo, E. Altshuler, M. Stiber, and A. Garfinkel, "Periodic inhibition of living pacemaker neurons: II. Influences of driver rates and transients and of non-driven post-synaptic rates," *Int. J. Bifurcation and Chaos*, vol. 1, pp. 873–90, December 1991.

[7] J. Segundo, "What can neurons do to serve as integrating devices?," *J. Theoret. Neurobiol.*, vol. 5, pp. 1–59, 1986.

[8] J. Segundo, M. Stiber, E. Altshuler, and J.-F. Vibert, "Transients in the inhibitory driving of neurons and their post-synaptic consequences," *Neuroscience*, vol. 62, no. 2, pp. 459–80, 1994.

[9] M. Stiber, *Dynamics of Synaptic Integration.* PhD thesis, University of California, Los Angeles, 1992.

[10] M. Stiber and J. P. Segundo, "Dynamics of synaptic transfer in living and simulated neurons," in *IEEE International Conference on Neural Networks*, (San Francisco), pp. 75–80, 1993.